Effect of nanocrystalline structure on magnetocaloric effect in manganite composites (1/3) La$_{0.7}$Ca$_{0.3}$MnO$_3$ / (2/3) La$_{0.8}$Sr$_{0.2}$MnO$_3$

M. Pękała[1], K. Pękała[2], V. Drozd[3], J.-F. Fagnard[4], P. Vanderbemden[4]

[1]Department of Chemistry, University of Warsaw, Al. Żwirki i Wigury 101, PL-02-089 Warsaw, Poland, pekala@chem.uw.edu.pl

[2]Faculty of Physics, Warsaw Technical University, PL-00-662 Warsaw, Poland

[3]Center for Study Matter at Extreme Conditions, Florida International University, Miami, FL 33199, USA

[4]SUPRATECS, Department of Electrical Engineering and Computer Science (B28), University of Liège, B-4000 Liège, Belgium

Abstract

Poly- and nanocrystalline manganite composites (1/3)La$_{0.7}$Ca$_{0.3}$MnO$_3$ and / (2/3)La$_{0.8}$Sr$_{0.2}$MnO$_3$ prepared by the sol-gel method are studied by magnetic and transport measurements. The Arrott plots and universal curve of magnetic entropy change confirm that magnetic transition is of the second order. The magnetocaloric effect of polycrystalline composite is found to be roughly twice smaller as compared to the polycrystalline Ca- and Sr-based parent phases. The nanocrystalline composite of the same composition exhibits only 8 % reduction of magnetic entropy change. Due to the large temperature spread of magnetocaloric effect the relative cooling power RCP of nanocrystalline composite is about three times larger as compared to the nanocrystalline Ca- and Sr- based parent phases. The maximum magnetic entropy change DS$_{MAX}$ and relative cooling power RCP are found to be more sensitive to magnetic field strength for the nano- than for polycrystalline composites studied.

Introduction

The magnetic refrigeration is known to be a more energy efficient and environmental friendly technology as compared with the traditional gas compression refrigeration technology [1]. This technology is based on the magnetocaloric effect (MCE) which is the reversible temperature response of a magnetic material to a change of external magnetic field.

Upon the application or removal of magnetic field the entropy is exchanged between the magnetic and lattice subsystems, which results in temperature change of material [2]. The magnetocaloric effect comes into a play in vicinity of ferro- to paramagnetic transition at the Curie temperature.

Many efforts have been made in a search for new materials exhibiting the relatively strong magnetocaloric effect close to the room temperature, which are suitable for potential applications. For the efficiency reason the ideal magnetocaloric material is expected to exhibit the so called "table-like" magnetic entropy changes, which ensures the maximum cooling power (RCP). Recently the mixed valence perovskite manganites have attracted increasing interests since some of them are cheap, chemically stable, easy to prepare and their physical parameters may be tuned by various methods of microstructural modification, including the composite systems too [3-7]. Moreover, the manganites are known to exhibit a negligible magnetic hysteresis.

The mixed valence state is generated by a substitution of the trivalent rare earth ions with the divalent or monovalent ones. The partial doping converts the Mn^{3+} ions to Mn^{4+} , which varies a ratio r_A/r_B of mean radii of cationic A and B sites. Furthermore, this affects the crystallographic structure and modifies materials properties. This modulates the distances between the manganite sites as well as the Mn-O-Mn angles responsible for the exchange interaction. The ferromagnetic interactions and electronic transport processes in manganites have been mainly explained by the hopping of the itinerant e_g electron via the Mn^{3+}–O^{2-}–Mn^{4+} bond, which can be affected by the ratio of Mn^{3+}/Mn^{4+} and the one-electron bandwidth. Thus, the Curie temperature may be tuned by a proper doping.

Beyond the relatively large magnetic entropy change in moderate magnetic fields, the magnetocaloric material is expected to reveal a broad temperature interval over which magnetocaloric effect spreads. This temperature width is determined by a sharpness of the magnetic transition. The magnetocaloric effect is known to depend on materials microstructure which controls a sharpness of magnetic transition. This opens a possibility to modify magnetocaloric properties for practical applications in magnetic refrigeration systems. The size reduction down to a nanometric scale is known to strongly rearrange the magnetic and electronic properties that become different from their bulk and film counterparts. It was observed that a transition from bulk material to the nanostructured one and / or to the low dimensional structure broadens the temperature width. A variety of ways were tested in order to tailor materials parameters suitable for magnetic refrigeration systems [7-9].

This paper continues and extends a search for the enhancement of the magnetocaloric effect itself and of the relative cooling power RCP in manganite systems. The underlying physical idea is to combine two materials with MCE peaks separated well enough. An overlap of MCE of both materials is expected to remarkably broaden the temperature width range, which in turn magnifies RCP. Recently this approach was tested for equal fractions (1:1) of $La_{0.7}Ca_{0.3}MnO_3$ and rhombohedral $La_{0.8}Sr_{0.2}MnO_3$ manganite phases [10]. Now it is checked for the 1:2 ratio of these phases. The magnetocaloric effect is additionally modified by changing a microstructure from polycrystalline to nanocrystalline one.

Experimental

The orthorhombic $La_{0.7}Ca_{0.3}MnO_3$ and rhombohedral $La_{0.8}Sr_{0.2}MnO_3$ manganites were produced by the sol-gel method, following a procedure described in [10].]. The starting reagents were La_2O_3, $Sr(NO_3)_2$, $CaCO_3$ and $MnCO_3$. Composites built of the $La_{0.7}Ca_{0.3}MnO_3$ and $La_{0.8}Sr_{0.2}MnO_3$ phases with a ratio 1:2 were prepared in a form of the polycrystalline and two nanocrystalline ones by annealing sol-gel precursor at 1250, 650 and 900°C, respectively.

X-ray powder diffraction was done using Bruker GADDS/D8 X-ray system with Apex Smart CCD Detector and direct-drive rotating anode. The MacSci rotating anode (Molybdenum) operates with a 50 kV generator and 20 mA current. The 2D diffraction patterns obtained were integrated using Fit2D and refined with GSAS-EXPGUI software package [11-12].

X-ray diffraction (XRD) pattern of lanthanum hexaboride standard of particle size 2 μm was used as the reference. Rietveld structure refinement was performed on the XRD patterns of the above mentioned materials using GSAS software. Refined value of Lorentzian Scherrer broadening term in GSAS profile function of LaB_6 was used as an instrumental broadening. This value was subtracted from the corresponding broadening term of the manganites to get diffraction lines broadening related to the particle size effect. Particle size was calculated by the formula:

$$P(\overset{0}{A}) = \frac{18000 * B * \lambda}{\pi * X} \tag{1}$$

where B is Scherrer constant (0.9), λ is X-ray radiation wavelength; X – Lorentzian Scherrer broadening term in GSAS profile function. Scanning electron microscopy images were obtained using JEOL JSM 5900LV instrument.

In order to facilitate a comparison with the previous investigation of a composite with phase ratio 1:1, the magnetic and resistivity measurements were made in the same conditions as the previous ones described in [10] . The AC susceptibility was measured at the amplitude of 10 Oe and frequency of 1053 Hz. Magnetization isotherms of up to H = 20000 Oe have been recorded in the broad temperature interval.

Structural characterization

XRD analysis showed that both $La_{0.7}Ca_{0.3}MnO_3$ and $La_{0.8}Sr_{0.2}MnO_3$ are single phase perovksites phases with orthorhombic and rhombohedral distortion of the crystal lattice, respectively. The unit cell parameters of the orthorhombic $La_{0.7}Ca_{0.3}MnO_3$ and rhombohedral $La_{0.8}Sr_{0.2}MnO_3$ manganites were found to be in good agreement with previously reported values [13-14].

Tab. 1 lists mean crystallite sizes of nanocrystalline composites, which increase from about 30 nm to about 130 nm, when a synthesis temperature varies from 650 °C to 900 °C. These crystallite sizes are comparable with those of the previously studied composites composed of equal fractions (1:1) of the same Ca and Sr based manganites [10]. The annealing temperature affects also the sizes of grains, which grow up agglomerating several crystallites. The SEM images (Fig. 1) show that mean estimated sizes of the multicrystallite grains are ca. 75 - 100 nm and 150 - 200 nm for the composites annealed at 650 °C to 900 °C, respectively. The grain sizes of composites studied are smaller as compared with manganites prepared by the solid state reaction. Moreover, the narrower distribution of grain sizes is typical for the sol-gel method.

Magnetic susceptibility

The temperature variation of the AC magnetic susceptibility reveals remarkable differences between the polycrystalline and nanocrystalline manganite composites (Fig. 2). The Sr and Ca based phases present in the polycrystalline composite may be clearly distinguished by the separated Curie temperatures derived from a derivative $d\chi'/dT$ and located about 303 K and 167 K, respectively. Moreover, the out-of-phase component χ'' is also enhanced around these temperatures. The SNC2 composite with relatively larger crystallites exhibits the χ' maximum about 70 K. The antiferromagnetic interactions are responsible for the low temperature fall in χ'. Temperature variation above 70 K is almost linear and the extrapolated χ' vanishes about 360 K. The χ'' component is spread over the

broad temperature interval between approximately 30 and 340 K. The high temperature χ' of SCN1 composites composed of smaller crystallites approaches zero about 360 K too. One may notice that the magnitude of χ' becomes reduced when passing from the polycrystalline composites to the nanocrystalline ones SNC2 and SNC1. The susceptibility reduction is due to the enhanced volume of the magnetically dead surface layer of the nanometer sized crystallites, which was discussed in [10,15].

Magnetization isotherms

The magnetization isotherms registered in magnetic fields up to 20000 Oe, plotted in Fig. 3, show the most abrupt magnetization increase occurring at low magnetic fields up to about 1000 Oe for both the polycrystalline and nanocrystalline SCN2 composites. The highest (but not a saturation) magnetization of 41 G cm^3/g is achieved by the polycrystalline composite at 242 K whereas the magnetization of 50 G cm^3/g is found for the SNC2 composite at 40 K. When comparing the isotherms at 300 K and at 20000 Oe , a magnetization of polycrystalline composite achieves 20 G cm^3/g whereas the magnetization of SCN2 achieves the lower value equal to only 6.5 G cm^3/g (Fig. 3). Such a magnetization reduction is characteristic for nanostructured ferromagnets and is due to the structural and magnetic disorder.

The considerable magnetization suppression of nanostructured composite is also seen when comparing the temperature variation of spontaneous magnetization of the poly- and nanocrystalline composites (Fig. 4). A shape of spontaneous magnetization of SCN2 composite may suggest a magnetic transition occurring over a broad temperature interval, which in turn may reveal a broad distribution of local Curie temperatures.

Arrott plots

The Arrott plots (M^2 vs H/M) are built transforming the magnetization isotherms of the poly- and nanocrystalline composites (Fig. 5). The positive slope observed for all temperatures studied indicates that the magnetic transition is of the second order [16]. The thermodynamic parameter A derived from Arrott plots (Fig. 6) enables to determine the Curie temperatures, which are equal to 296 K and 233 K for the polycrystalline and SCN2 composites, respectively. In a case of polycrystalline composite the T_C is only 7 K lower than the T_C derived from magnetic susceptibility, which corresponds to the Sr rich phase. The $T_C =$ 233 K of the SCN2 composite seems to arise from a broad distribution of local Curie temperatures of the strongly disordered nanocrystalline SCN2 composite.

Magnetocaloric effect

The magnetic entropy change was determined indirectly from measured magnetization isotherms using the Maxwell relation [17]. Temperature variation of the magnetic entropy change, DS(T), exhibits distinct features for the poly- and nanocrystalline composites, as plotted in Fig. 7. For 2 T change in magnetic field, the polycrystalline composite exhibits the DS maximum (equal to maximum negative change of magnetic entropy) almost equal to -1 J/kg K at 300 K whereas the DS maximum slightly exceeding -0.4 J/kg K is observed at 120 K for the nanocrystalline SCN2 composite.

For the polycrystalline composite the absolute low temperature slope of DS(T) is roughly three times smaller as compared to the high temperature slope. The similar slope ratio 1:2 was previously seen for the polycrystalline composite of equal fractions of $La_{0.7}Ca_{0.3}MnO_3$ and $La_{0.8}Sr_{0.2}MnO_3$ [10]. The inverse relation of DS slopes is found for the nanocrystalline composite. Namely, the low temperature slope is 2.5 times higher than the high temperature one.

For the polycrystalline composite built of the $La_{0.7}Ca_{0.3}MnO_3$ and $La_{0.8}Sr_{0.2}MnO_3$ phases with a ratio 1:2, the maximum magnetic entropy change DS_{MAX} is approximately twice reduced as compared with the polycrystalline parent Sr- and Ca- based manganite phases (Fig. 8). For the corresponding nanocrystalline composite the DS_{MAX} is only up to 8 % smaller than for the nanocrystalline parent Sr- and Ca- based manganite phases.

The maximum entropy change appears at temperature, where the temperature variation of magnetization is most abrupt. The magnitude of maximum entropy change DS_{MAX} increases exponentially with the magnetic field change according to $\sim H^N$. Values of the N exponent equal to N = 0.93 ± 0.015 and 1.1 0± 0.015 for the poly- and nanocrystalline composites, respectively. The higher sensitivity of DS to magnetic field is characteristic for the nanocrystalline manganites and was previously observed for similar systems [10, 18].

The temperature half width, δT, measures a spread of magnetocaloric effect and corresponds to the temperature interval, in which a heat may be transported in the direction opposite to temperature gradient. A more detailed inspection indicates the distinct variation of δT in poly- and nanocrystalline composites. In the polycrystalline composite the δT broadens from 74 K at 0.5 T to 85 K at 2 T. The corresponding cooling power, RCP, reaches 82 J/kg for 2 T magnetic field for the polycrystalline composite. In the nanocrystalline composite δT is much broader but it varies only between 220 and 225 K for magnetic field varying from 0.5

and 2 T. This remarkably broad temperature half width, δT, causes that the relative cooling power RCP of studied nanocrystalline composites reaches 93 J/kg for 2 T magnetic field. This RCP is roughly three times larger as compared with nanocrystalline parent Sr- and Ca- based manganite phases (Fig. 9).

Fig. 9 compares the RCP values of the poly- and nanocrystalline composites studied (1:2 ratio) with the previous investigation for 1:1 ratio [10] and with the pure $La_{0.7}Ca_{0.3}MnO_3$ and $La_{0.8}Sr_{0.2}MnO_3$ phases. One may notice that the parent phases were prepared by the similar method since the magnetocaloric effect is known to be sensitive to the microstructure created by the specific production and treatment methods. In contrast to polycrystalline composite one may see the remarkable enhancement of RCP occurring for both nanocrystalline composites with 1:1 and 1:2 ratio of $La_{0.8}Sr_{0.2}MnO_3$ phase, as compared to the Sr and Ca based parent manganites. The highest value of RCP is found for the nanocrystalline composite with phase ratio 1:2 (Fig. 9). This RCP exceeds the RCP values of the both polycrystalline composites with 1:1 and 1:2 ratio. Thus, the relative cooling power may be tuned by controlling the crystallite mean sizes of manganites annealed at various temperatures and time periods, which will be investigated separately.

The dependence of RCP magnitude on magnetic field strength may be accounted for by the exponential formula $\sim H^R$. The derived values of R exponent are equal to 1.03 ± 0.007 and 1.12 ± 0.017 for the poly- and nanocrystalline composites, respectively, and reveal the enhanced sensitivity of nanocrystalline composite. A simple analysis of this exponential dependence shows that the RCP = 82 J/kg found kg for 2 T magnetic field for the polycrystalline composite may attained in nanocrystalline composite only at a magnetic field of 1.77 T. This demonstrates the superior features of nanocrystalline composites and points to a possible enhancement of magnetic field sensitivity of these materials, when creating the optimum microstructure using a proper heat treatment.

Universal curve of magnetic entropy change

In order to additionally check an order of the magnetic phase transition the so called universal curves of magnetic entropy change $S_R(\theta)$ are constructed according to

$$S_R(\theta) = DS(T) / DS_{MAX}, \qquad (2)$$

where

$$\theta = - (T - T_C) / (T_L - T_C) \qquad \text{for } T \leq T_C$$

$$\theta = (T - T_C) / (T_R - T_C) \qquad \text{for } T_C \leq T$$

where T_L and T_R denote the low and high temperature reference temperatures corresponding to a half of DS_{MAX} [1]. Fig. 10 shows that the universal curves measured in various magnetic fields up 2 T clearly coincide in the whole temperature range investigated both for the poly- and nanocrystalline composites. This proves the second order phase transition, which is consistent with the Arrott plots (above). The relatively enhanced scatter observed for the nanocrystalline composite is related to smaller absolute values of measured magnetic entropy change.

Electrical resistivity and magnetoresistance

Electrical resistivity of the nanocrystalline composites studied reaches about 0.08 to 0.10 Ωm at room temperature. The absolute resistivity values are determined with 10 % accuracy limited by a shape irregularity. At lowest temperature of 22 K the resistivity achieves 1.7 and 1.1 Ωm for the SCN1 and SCN2 composites, respectively. This points to the relatively higher residual resistivity of SCN1 composite containing finer crystallites. The shallow resistivity minimum seen about 40 to 50 K (Fig. 11) is related to the spin dependent charge carrier tunneling/scattering on grain boundaries between antiferromagnetically coupled grains. The resistivity maximum revealing a transition between the low temperature metallic like phase and the high temperature semiconducting one is located at 45 and 115 K for the SCN1 and SCN2 composites, respectively.

An application of the 1 T magnetic field shifts slightly the resistivity maxima towards higher temperature and suppresses the resistivity. For $\rho(T,B)$ and $\rho(T,0)$ denoting a resistivity measured with and without magnetic field, respectively, the magnetoresistance (MR) effect defined as

$$MR(T) = \rho(T,B) / \rho(T,0) - 1 \qquad\qquad (3)$$

is plotted in Fig. 12, showing that MR raises monotonically from a few percent close to the room temperature to almost -50 % around 30 K. One can see only a minute differences between the both nanocrystalline composites studied. The positive slope seen in the

temperature dependence confirms that the negative magnetoresistance is of the extrinsic type being related to the electron spin dependent tunneling between crystallite/grains and/or scattering of electrons in the disordered surface layers [19].

Conclusions

In summary, we have systematically investigated the physical properties of nano- and polycrystalline manganite composites $(1/3)La_{0.7}Ca_{0.3}MnO_3$ and / $(2/3)La_{0.8}Sr_{0.2}MnO_3$. The Arrott plots and universal curve of magnetic entropy change confirm that magnetic transition is of the second order. The magnetic entropy change of polycrystalline composites is found to be roughly twice smaller as compared to the polycrystalline Ca- and Sr- based parent phases. The nanocrystalline composite of the same composition exhibits only 8 % reduction of magnetic entropy change. Due to the large temperature spread of magnetocaloric effect the relative cooling power RCP of nanocrystalline composite is about three times larger as compared to the nanocrystalline Ca- and Sr- based parent phases.

The maximum magnetic entropy change DS_{MAX} and relative cooling power RCP are found to be more sensitive to moderate magnetic field strength for the nano- than for polycrystalline composites studied. A magnitude of electrical resistivity ensures that the eddy currents generated in manganite composites may be limited. These observations confirm that the magnetocaloric materials with the more competitive properties may be developed in a form of nanocrystalline composites.

References

1. V. Franco, J.S. Blazquez, B. Ingale, A. Conde, Annu. Rev. Mater. Res. 42 (2012) 305

2. J.S. Amaral, V.S.Amaral, Journal of Magnetism and Magnetic Materials 322 (2010) 1552

3. T. Zhang, X.P. Wang, Q.F. Fang, X.G. Li, Appl. Physics Reviews 1 (2014) 031302

4. M.H. Phan, S.C. Yu, J. Magn. Magn. Mater. 308 (2007) 325

5. P. Lampen, N.S. Bingham, M.H. Phan, H. Kim, M. Osofsky, A. Pique, T.L. Phan, S.C. Yu, H. Srikanth, Appl. Phys. Lett. 102 (2013) 062414

6. M. Kumaresavanji, C.T. Sousa, A. Pires, A.M. Pereira, A.M. L. Lopes, J.P. Araujo, Appl. Phys. Lett. 105 (2014) 083110

7. P. Alvarez, J.L.Sanchez Llamazares, P. Gorria, J. A. Blanco, Appl. Phys. Lett. 99 (2011) 232501

8. R. Caballero-Flores, V. Franco, A. Conde, K.E. Knipling, M.A. Willard, Appl. Phys. Lett. 98 (2011) 102505

9. A. Chaturvedi, S. Stefanoski, M.H. Phan, G.S. Nolas, H. Srikanth, Appl. Phys. Lett. **99 (**2011) 162513

10. M. Pękała, K. Pękała, V. Drozd, K. Staszkiewicz, J.-F. Fagnard, P. Vanderbemden, Journal of Applied Physics 112 (2012) 023906 (1-9)

11.Toby BH. EXPGUI, a graphical user interface for GSAS. J. Appl. Cryst. 2001;34:210-221;

12. Larson C, Von Dreele RB. General Structure Analysis System (GSAS): Los Alamos National Laboratory Report LAUR, 2000. P.86-748

13. M. Pękała, N. Kozlova, V. Drozd, Journal of Applied Physics 104 (2008) 123902

14. M. Pękała, V. Drozd, J. Non-Crystalline Solids 354 (2008) 5308

15. J. Curiale, M. Granada, H.E. Troiani, R.D. Sánchez, A.G. Leyva, P. Levy, K. Samwer, Appl. Phys. Lett. 95 (2009) 043106

16. S.K. Banerjee, Phys. Lett. 12 (1964) 67

17. R. Caballero-Flores, N.S. Bingham, M.H. Phan, M.A. Torija, C. Leighton, V. Franco, A. Conde, T.L. Phan, S.C. Yu, H. Srikanth, J. Phys.: Condens. Matter 26 (2014) 286001

18. M. Pękała, Journal of Applied Physics 108 (2010) 113913 (1-4)

19. G. Venkataiah, P. Venugopal Reddy, J. Magn. Magn. Mater. 285 (2005) 343.

Figures
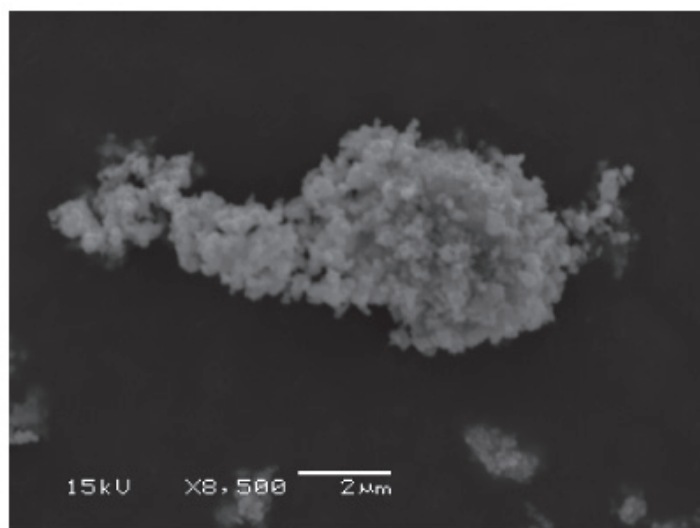
Fig 1A
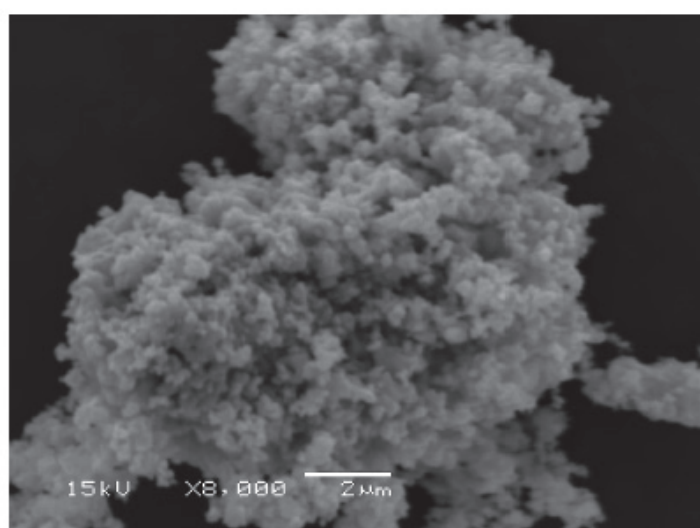
Fig 1B

Fig. 1. SEM images of composite samples annealed at 650 ºC (A) and 900 ºC (B).
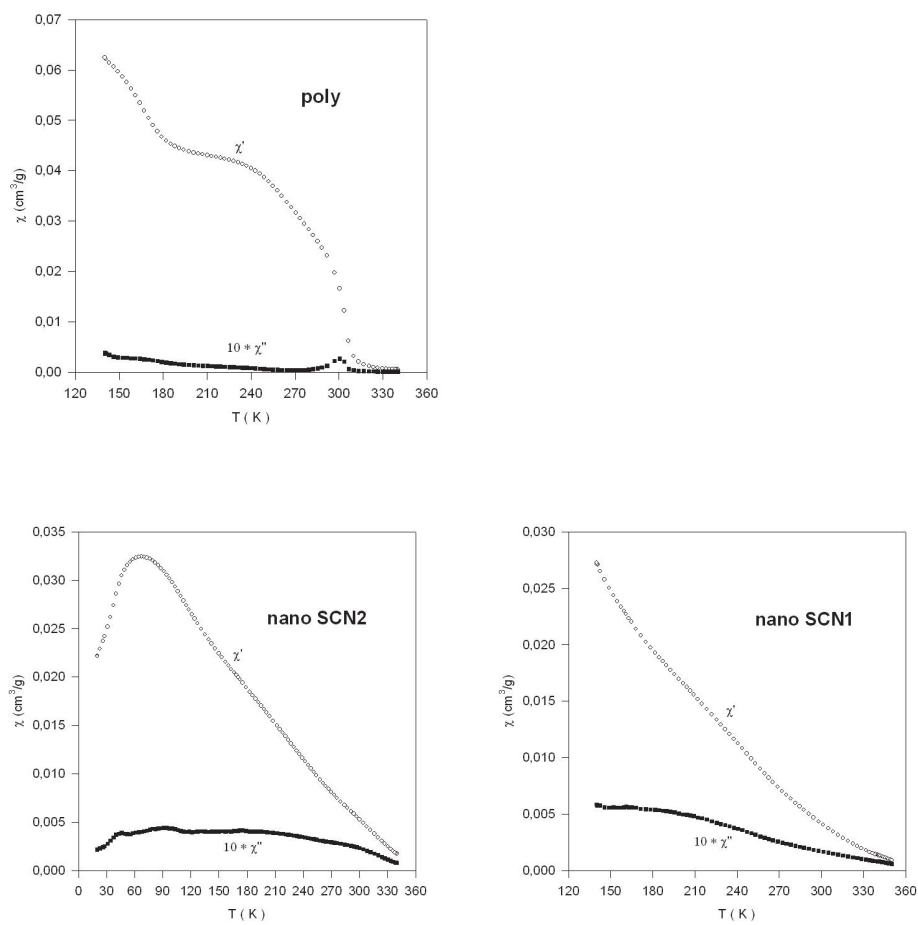
Fig. 2. Temperature variation of in-phase and out-of-phase magnetic susceptibility of polycrystalline (A), nanocrystalline (SCN2) (B) and nanocrystalline (SCN1) (C) composites.
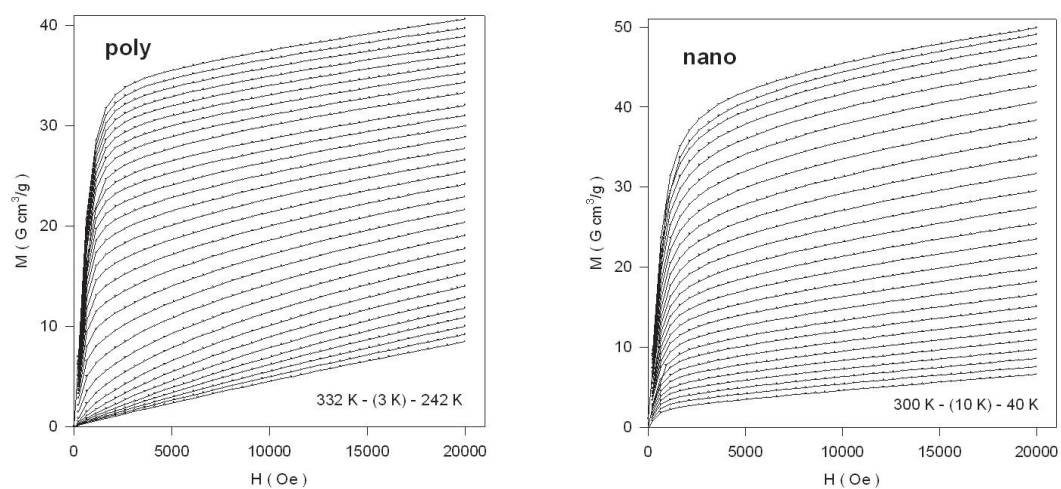
Fig. 3. Magnetization isotherms of polycrystalline (A) and nanocrystalline (B) composites.
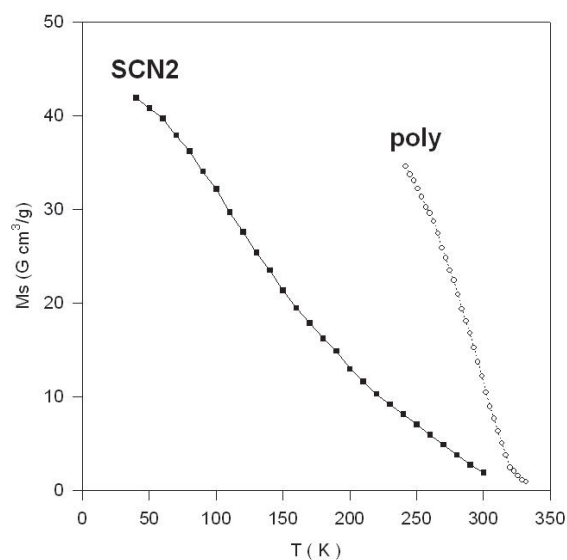
Fig. 4. Temperature variation of spontaneous magnetization of polycrystalline and nanocrystalline composites.
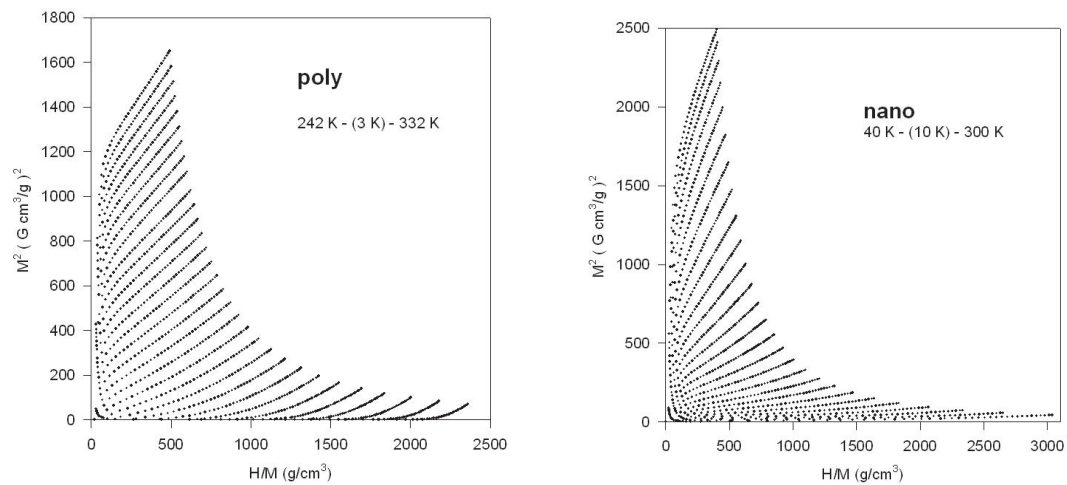
Fig. 5. Arrott plots of polycrystalline (A) and nanocrystalline (B) composites, in temperature intervals 242 – 332 K and 40 – 300 K, respectively.
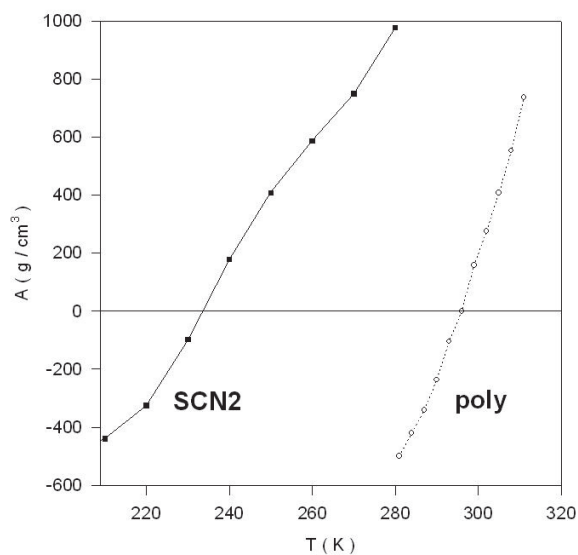
Fig. 6. A. Temperature variation of the thermodynamic A parameter of polycrystalline and nanocrystalline composites.
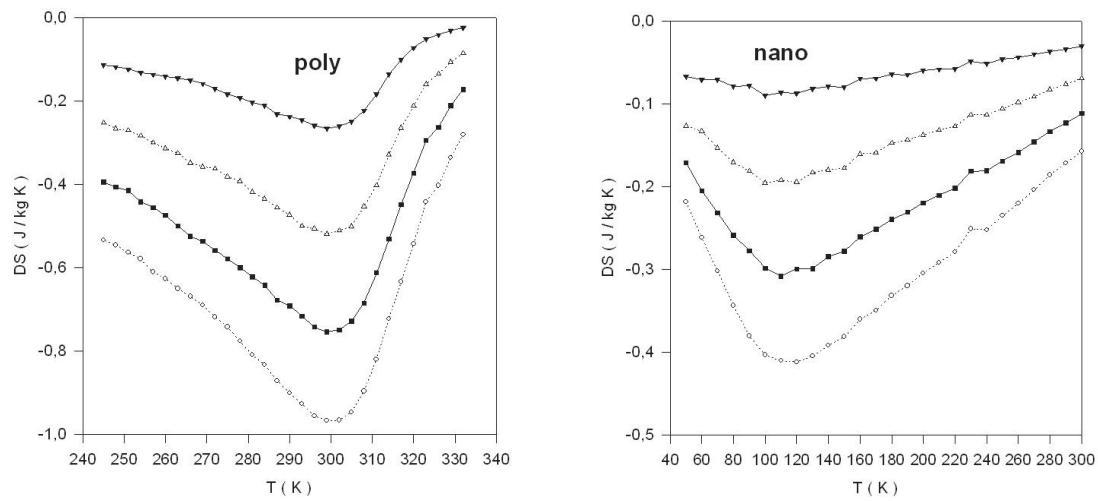
Fig. 7. Temperature variation of the magnetic entropy change for polycrystalline (A) and nanocrystalline (B) composites at a magnetic field change of 0.5, 1.0, 1.5 and 2.0 T (from top to bottom).
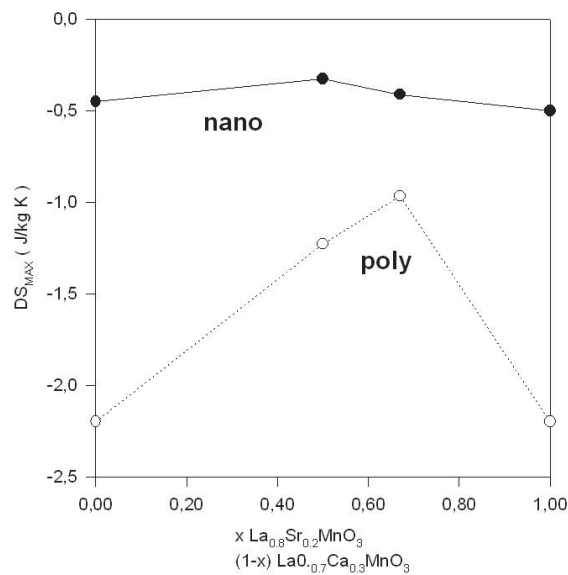
Fig. 8. Maximum magnetic entropy change for magnetic field of 2 T as a function of $La_{0.8}Sr_{0.2}MnO_3$ phase fraction in polycrystalline and nanocrystalline composites.
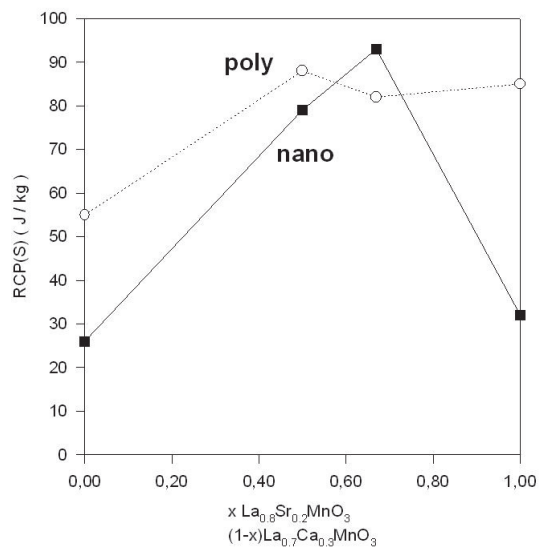
Fig. 9. Relative cooling power for magnetic field of 2 T as a function of $La_{0.8}Sr_{0.2}MnO_3$ phase fraction in polycrystalline and nanocrystalline composites.
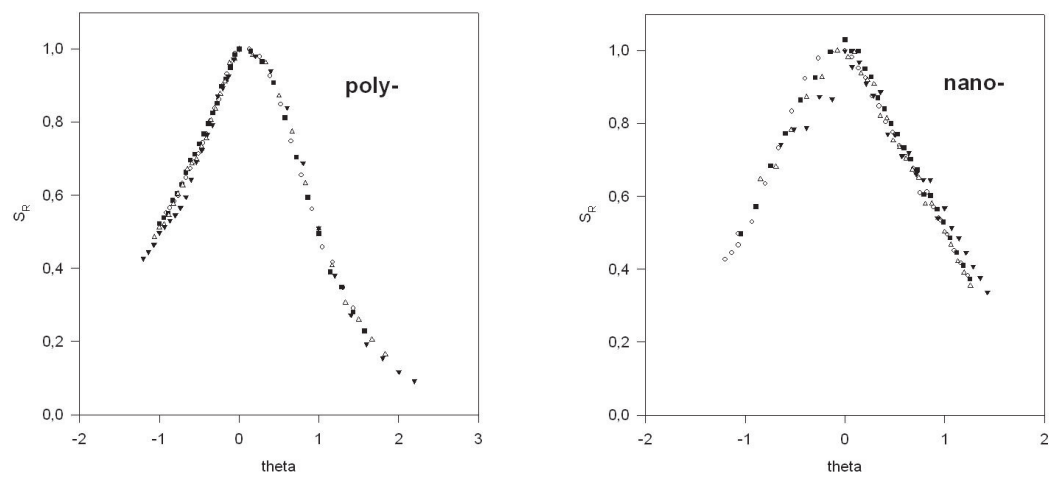
Fig. 10. Universal curve of normalized magnetic entropy change as a function of reduced temperature for the polycrystalline (A) and nanocrystalline (B) composites.
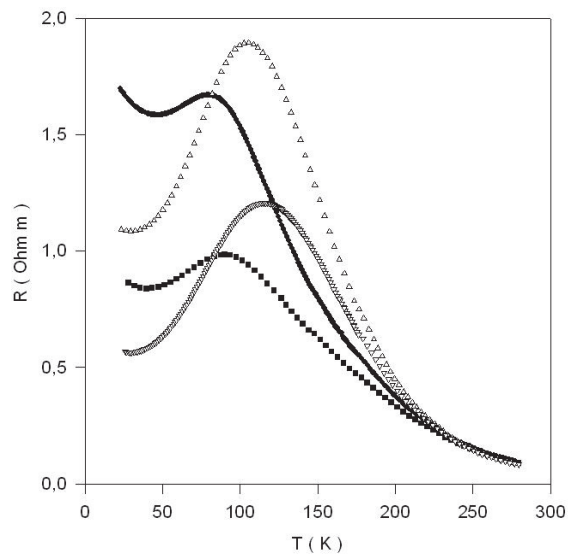
Fig. 11. Temperature variation of electrical resistivity of the SCN1 (solid symbols) and SCN2 (open symbols) nanocrystalline composites at zero and 1 T magnetic field.
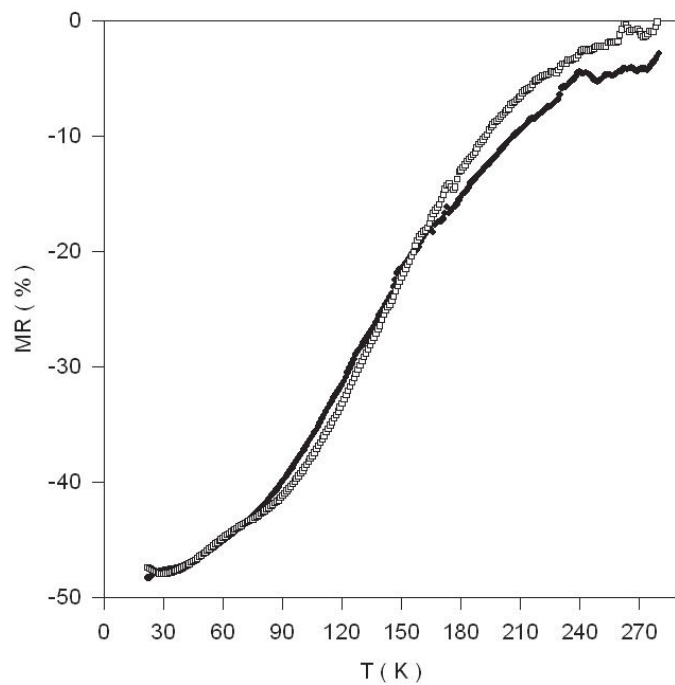
Fig. 12. Temperature variation of magnetoresistance at 1 T magnetic field for the SCN1 (solid symbols) and SCN2 (open symbols) nanocrystalline composites.

Table 1. Mean crystallite sizes of nanocrystalline composites synthesized at 650 and 900 ^{o}C.

Composition	SCN1-crystallite size @650°C (nm)	SCN2-crystallite size @900°C (nm)
La$_{0.7}$Ca$_{0.3}$MnO$_3$	33	135
La$_{0.8}$Sr$_{0.2}$MnO$_3$	27	126